International Journal of Pharmaceutics 637 (2023) 122895

Contents lists available at ScienceDirect

International Journal of Pharmaceutics

journal homepage: www.elsevier.com/locate/ijpharm

Manipulating drug release from 3D printed dual-drug loaded polypills using challenging polymer compositions

Thomas McDonagh [a], Peter Belton [b], Sheng Qi [a,*]

[a] School of Pharmacy, University of East Anglia, Norwich, UK
[b] School of Chemistry, University of East Anglia, Norwich, UK

ARTICLE INFO

Keywords:
3D printing
Polypill
Controlled drug delivery
Solid dispersions
Arburg plastic freeforming
Fused deposition modelling
Tablet design principle

ABSTRACT

Combining multiple medications in a single dosage form has emerged as an important strategy for treating complex diseases and could help tackle the growing issue of polypharmacy. In this study we investigated the suitability of different dual-drug designs for achieving simultaneous, delayed and pulsatile drug release regimes using two model formulations: an immediate release erodible system of Eudragit E PO loaded with paracetamol; and an erodible swellable system of Soluplus loaded with felodipine. Both binary formulations, despite not fused deposition modelling (FDM) printable, were successfully printed using a thermal droplet-based 3D printing method, Arburg Plastic Freeforming (APF), and exhibited good reproducibility. X-ray powder diffraction (XRPD), Attenuated Total Reflectance Fourier Transform Infrared Spectroscopy (ATR-FTIR) and Differential Scanning Calorimetry (DSC) were used to assess drug-excipient interaction. The printed tablets were evaluated for drug release using *in vitro* dissolution testing. We found the simultaneous and delayed release designs were effective at generating the intended drug release profiles, giving insight into the types of dual-drug designs which can be used to create complex release profiles. In contrast the pulsatile tablet release was non-defined, highlighting the design limitations when using erodible materials.

1. Introduction

Combining multiple medications in a single dosage form has emerged as an important strategy for tackling the growing issue of polypharmacy, defined as the use of five or more medications daily by an individual (Vaz and Kumar, 2021; Roshandel et al., 2019) and for treating complex diseases (Bangalore et al., 2007; Gao et al., 2014; Roshandel et al., 2019). Polypharmacy is becoming increasingly common, especially in elderly populations and is a known risk factor associated with increased mortality due to poor adherence and the adverse effect of antagonistic drug interactions (Pasina et al., 2014; Rodrigues and Oliveira, 2016). Furthermore many complex diseases, such as rheumatoid arthritis, cardiovascular disorders, bronchial asthmas, cancer, and some neurological disorders are regulated by the human circadian rhythm, requiring drug administration at certain times of the day (Mandal et al., 2010). Therefore, multi-active dosage forms that offer more sophisticated or modified/pulsatile release and can synchronise with the circadian rhythm and the symptomology of such diseases are desirable, providing the prospect for improved treatment effectiveness (Dumpa et al., 2018). Whilst several fixed-dose combination polypills (i.e. personalised fixed-dose combination of more than one drugs) have been commercialised using traditional manufacturing techniques (T.I.P. Study, 2009; Wiley and Fuster, 2014) there has been limited uptake, mainly because of the inability to individualise the therapy due to inflexible manufacturing (Power of one, 2019; Robles-Martinez et al., 2019).

Additive manufacturing (AM) has been widely researched for single drug personalised medicine showing a lot of promise not only for drug dose tuning (by modifying the volume of deposited drug loaded material) (McDonagh et al., 2022; Cui et al., 2021; Herrada-Manchón et al., 2020) but also for complex release tuning, using software parameters such as infill density to modify the release properties of the printed tablets (McDonagh et al., 2022; Martinez et al., 2018; Zhang et al., 2021; Zhang et al., 2021; Korte and Quodbach, 2018; Zhang et al., 2017; Chew et al., 2016). Dual-drug and multi-API tablet 3DP manufacture has been partially explored in the literature. In these studies, semi-solid extrusion (SSE) AM is the most commonly employed 3D printing method (Goh et al., 2021; Alayoubi et al., 2022; Khaled et al., 2015; Zhang et al., 2022), but thermal based printing techniques may be more desirable for point of care small batch production as no post processing drying step

* Corresponding author.
E-mail address: sheng.qi@uea.ac.uk (S. Qi).

https://doi.org/10.1016/j.ijpharm.2023.122895
Received 3 January 2023; Received in revised form 17 March 2023; Accepted 24 March 2023
Available online 25 March 2023

required. However thermal 3D printing, most commonly used being fused deposition modelling (FDM), requires the drug to be thermally processed into filaments as the feedstock prior to the thermal printing step. In practice, this approach faces three key challenges: (1) most pharmaceutical polymers are not directly printable, thus plasticisers as the processing aid are needed which affect the *in vivo* performance of the product; (2) high risk of drug degradation as the drug is twice thermally processed; (3) time consuming with the filament making (which is not an established pharmaceutical manufacturing process at an industrial scale) and printing dual-step process. Direct powder extrusion is another thermal 3D printing technique that have been developed to simplify the manufacturing process and avoid twice-thermal processing of the materials (Goyanes et al., 2019; Boniatti et al., 2021; Sánchez-Guirales et al., 2021 Sep 29; Triastek, 2015). In reported direct powder extrusion literature, the powder feedstock is directly extruded and fed to the printing nozzle to be discharged. However, powder feeding and print quality can still be an issue when using challenging materials with high melt viscosities.

We recently developed a direct granule fed thermal droplet-based 3D printing process for tablet manufacture using Arburg plastic freeforming (APF). APF is a novel thermal droplet deposition technique with two print heads which has shown promise for its highly controllable, versatile material processing. Using APF, it is possible to process pharmaceutical materials which are impossible to print by other commercial thermal 3D printing techniques with good tablet quality, performance and reproducibility outcomes (McDonagh et al., 2022; McDonagh et al., 2022; Von Zeppelin and Manka, 2017). This new process directly addresses the challenges faced by other thermal 3D printing methods mentioned above. (1) It allows multi-drug loaded tablets to be printed without additives, simplifying tablet composition and controlled drug release variables. (2) It reduces the thermal exposure of the drug to only printing step. (3) It employs granulation process for feedstock preparation which is one of the most widely used process in pharmaceutical industry. In this study we are particularly interested in utilising this new process in combination with novel tablet geometry design to explore the capability of using a pair of pharmaceutical polymers with distinctively different properties to control independently the drug release kinetics of two drugs from a single tablet.

In this paper we demonstrate the use of APF printing to print dual-drug fixed-dose tablets for the first time. Eudragit E PO and Soluplus were chosen as model carrier polymers for tablet printing due to their challenging material processing properties (high brittleness and melt viscosity) (Yang et al., 2021) and solubility enhancement properties for poorly water soluble API (Saydam and Takka, 2020; Zhang et al., 2017; Heer et al., 2013). By precisely controlling the location of each formulation within the printed tablets we printed several dual-drug tablet designs targeting four pharmaceutically relevant release profiles: simultaneous release of two API; immediate release of one API, delayed release of second API; pulsatile release of alternate API. The results bring new insights regarding the design principles of dual-drug tablets with intended individualised drug release kinetics of each API.

2. Materials and methods

2.1. Materials

Eudragit E PO (Eud) was donated by Evonik (Evonik Industries, Germany), Soluplus (Sol) was donated by BASF (BASF, Germany), Paracetamol (Pac) was purchased from Molekula (Molekula Ltd, United Kingdom), and Felodipine (Felo) was purchased from Sigma Aldrich (Sigma Aldrich, United Kingdom).

2.2. Feed stock (granules) preparation

The granulated feedstocks were prepared using a wet granulation process. Two model drugs were used, paracetamol (Pac) and felodipine (Felo). Two types of granules were prepared loaded with the model drugs, Pac with Eudragit E PO (Eud) and Felo with Soluplus (Sol). For both granule formulations, a drug: polymer ratio of 1:10 (w/w) was used giving a drug loading of 9.1% (w/w). The polymer and drug were accurately weighed and mixed. The powder mixes were blended in a food mixer (Kenwood, UK) with flat beater attachment for 5 min prior to the addition of granulation fluid, Milli-Q water, which was followed by 15 min mixing until a 'sandy' consistency of the mixture was achieved. Wet granules were removed from the food mixer and tray-dried in an oven at 40 °C overnight to achieve<1% (w/w) moisture content. The dried granules were passed through sieves and the granules within 850 μm to 2 mm in size were used as the feedstock for APF printing (McDonagh et al., 2022).

2.3. APF printing of tablets

An Arburg Plastic Freeformer (APF) equipped with 2 piezo actuated thermal extrusion heads (200 μm nozzle diameter) was used for printing the drug loaded tablets. The details of instrumentation, material qualification and printing process were explained in our previous publication (McDonagh et al., 2022). Digital CAD files for the 3D geometries were generated in SOLIDWORKs and exported to Arburg proprietary slicing software (Freeformer software V2.2, Arburg, Germany) as an STL file. Cylindrical tablets were printed with dimensions 15 mm in diameter and 6 mm height with different designs. Printing conditions for each feed material are shown below in Table 1. Print speeds were 80 mm/s for the tablet contour and 40 mm/s for the infill region resulting in print times of approximately 3–4 min per tablet.

2.4. Dual-drug tablet designs

All printed dual-drug tablets had the same macro geometry (15 mm Diameter, 6 mm height) but varied design to achieve different release profiles (Fig. 1). Three types of drug release were targeted, Simultaneous release, Delayed release and Pulsatile release. In Simultaneous (Sim) release designs, denoted Sim1, Sim2 and Sim3 both materials, Eud-Pac and Sol-Felo are partially exposed at t = 0 during dissolution and so are readily available for dissolution. Delayed (Delay) release tablets denoted Delay1 and Delay2 are based on a core/shell design with a shell thickness of 1.2 mm. As such only the shell material is initially exposed at the start of the dissolution. Pulsatile release tablets were similar, designed and printed with concentric layers of alternate material with a material layer thickness of 0.6 mm.

2.5. Differential scanning Calorimetry (DSC)

A DSC2500 (TA Instruments, Newcastle, United States) was used to detect glass transition temperatures (T_g) and melting peaks of the raw materials, physical blends, granules and printed samples. The samples were characterised using a heating rate of 10 °C/min, from 0 °C to 200 °C. Aluminium standard TA crimped pans and lids (TA Instruments, Newcastle, USA) and sample weight of 2–5 mg were used. All tests were performed in triplicate.

2.6. Attenuated total reflectance Fourier transform infrared spectroscopy (ATR-FTIR)

A Vertex 70 FTIR spectrometer (Bruker Optics Ltd., United Kingdom) equipped with a Golden Gate, heat-enabled Attenuated Total Reflectance (ATR) accessory (Specac Ltd., Orpington, United Kingdom) fitted with a diamond internal reflection element was used to perform all ATR-FTIR measurements. All ATR-FTIR spectra were acquired in absorbance mode, using a resolution of 4 cm^{-1}, 128 scans, within 4000 cm^{-1} to 600 cm^{-1} wavenumbers. Spectra were analysed using OPUS version 7.8 (Bruker Optics Ltd., United Kingdom). All measurements were performed in triplicate.

Table 1
APF printing conditions for Eud-Pac and Sol-Felo tablets.

Feed material	Nozzle diameter (μm)	Temperatures (°C)			Build chamber temp. (°C)	Discharge (%)	Printing pressure (bar)	Aspect ratio (AR)	Layer height (mm)
		Zone 1	**Zone 2**	**Discharge nozzle**					
Eud-Pac	200	140	150	155	45	100	400–550	1.75	0.2
Sol-Felo	200	160	170	185	45	100	400	1.75	0.2

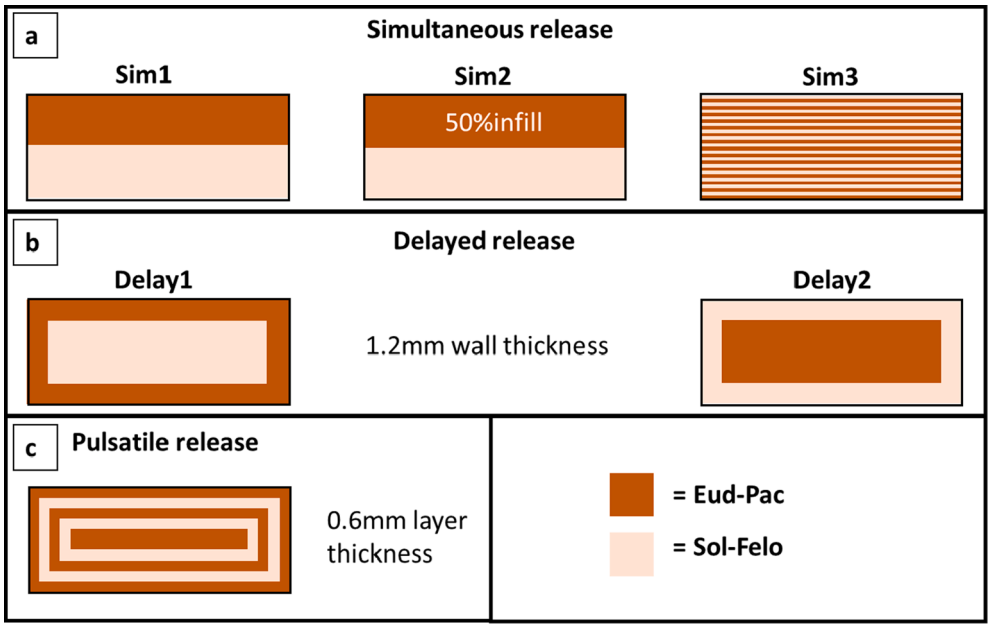

Fig. 1. Graphic illustrations of dual-drug tablet designs.

2.7. Powder X-ray diffraction (PXRD)

A SmartLab SE X-ray diffractometer (Rigaku, Tokyo, Japan) with monochromatic CuKα radiation (wavelength = 1.54056 Å) was used to collect the X-ray diffraction patterns of the raw materials, the granules and the APF printed tablets. For the printed samples, they were briefly ground to powder form prior to their measurements. All samples were measured with a scanning range of $5° < 2\theta < 60°$, a step width of 0.02° and a scan speed of 4°/minute.

2.8. Thermogravimetric analysis (TGA)

TGA was used to assess the thermal degradation temperatures of the raw materials to ensure formulations were processed below their degradation temperature. The samples (with a samples size of 5–10 mg) was loaded into aluminium pans and heated from 25 to 400 °C at 10 °C/min. All four raw materials showed no thermal degradation at temperatures below 200 °C.

2.9. Drug content measurement

Accurately weighed drug loaded printed Eud-Pac and Sol-Felo material was dissolved in a beaker containing 150 ml of dissolution media. 0.1 M pH 1.2 HCl was used for the Eud-Pac formulation and a 1:1 mixture of pH 6.8 phosphate buffer and ethanol was used for Sol-Felo formulation to maintain sink conditions. The beaker was covered with a parafilm tape to minimize solvent evaporation during dissolution. The medium was stirred using magnetic stirrer at room temperature. After complete dissolution, 1 ml samples were withdrawn. The samples were then scanned for their content of paracetamol or felodipine using a UV–VIS spectrophotometer (Perkin-Elmer lambda 35, USA) at 243 nm or 363 nm respectively. The loading efficiency measurements for the granules were carried out in triplicate.

2.10. In vitro drug release studies

The *in vitro* drug release profiles were measured in dissolution testing apparatus (Caleva 8ST, Germany) using the basket method (USP apparatus 1). A basket rotation speed of 100 rpm at 37 ± 0.5 °C were used for all measurements. Due to the poor solubility of Felo, 1% sodium dodecyl sulphate (SDS) was added to dissolution media to ensure sink conditions. For the first 2 h, tablets were placed in 900 ml of pH 1.2 HCl dissolution media with 1% SDS and subsequently transferred to 900 ml pH 6.8 phosphate buffer with 1% SDS for a further 22 h. 5 ml dissolution samples were withdrawn at pre-determined time intervals. The samples were directly filtered through a membrane filter with 0.45 μm pore size (Minisart NML single use syringe, Sartorius, UK). The samples were analysed using a UV–VIS spectrophotometer (CLARIOstar Plus, BMG Labtech) at 243 nm or 364 nm for paracetamol and felodipine respectively. All drug release studies were conducted in triplicate with the exception of the simultaneous release tablets which were done in duplicate.

3. Results and discussion

3.1. Physicochemical and thermal characterisation of APF printed tablets

Thermal and physiochemical characterisation using TGA, PXRD, ATR-FTIR and DSC was performed to understand how the model drugs were incorporated into the two polymer systems used in this study (Fig. 2). First, TGA analysis of the two API was conducted to establish their degradation profiles. The extrapolated onset degradation

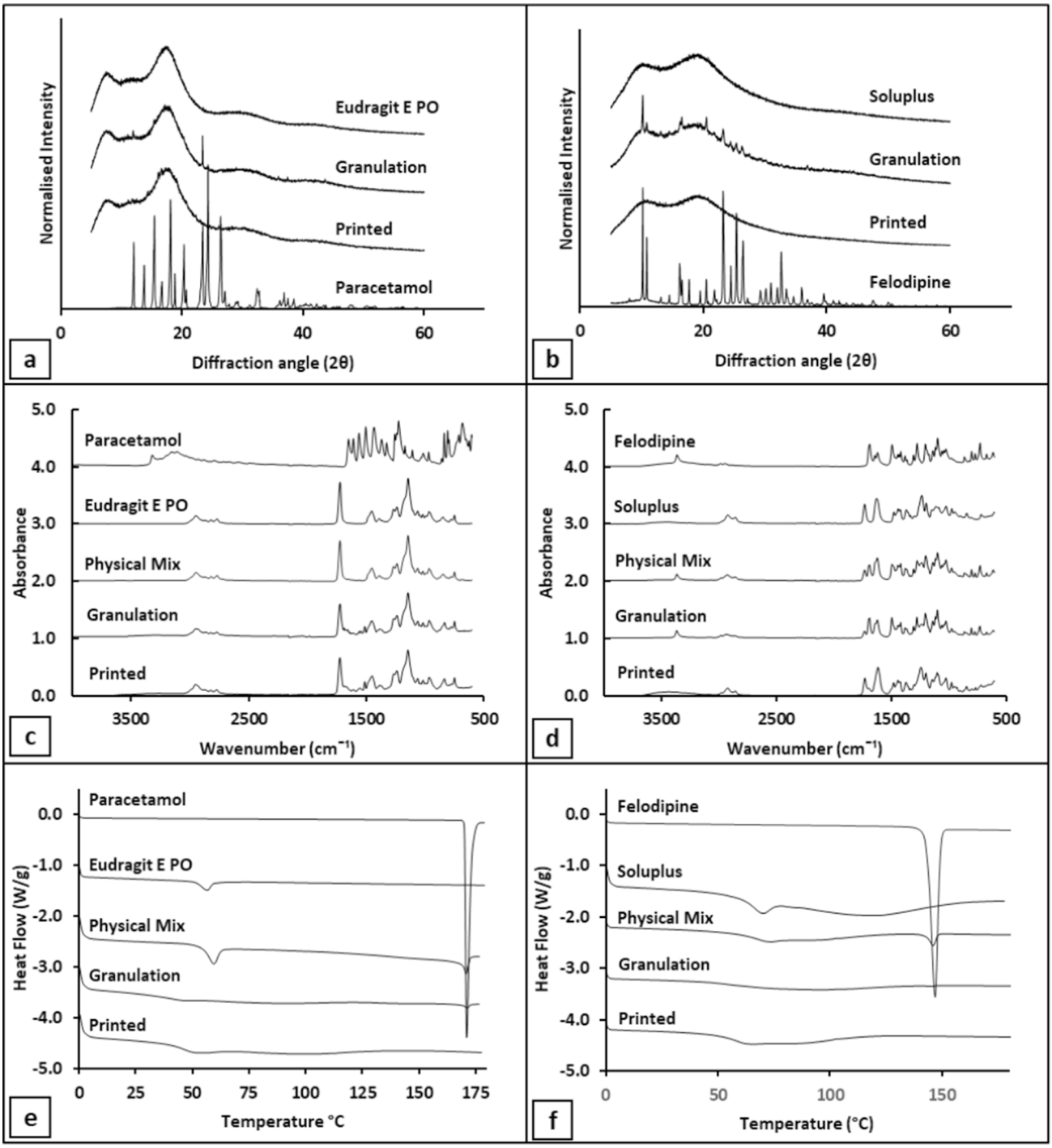

Fig. 2. Physiochemical characterisation of APF printed tablets and raw materials. PXRD diffraction patterns of the raw materials, granules and printed material for (a) the Eud-Pac formulation and (b) the Sol-Felo formulation. ATR-FTIR spectra of the raw materials, physical mix, granules and printed material for (c) the Eud-Pac formulation and (d) the Sol-Felo formulation. DSC thermograms of the raw materials, physical mix, granules and printed material for (e) the Eud-Pac formulation and (f) the Sol-Felo formulation.

temperature for Pac and Felo was 249 °C and 274 °C respectively. These temperatures are considerably higher than the conditions used during printing (155 °C for Eud-Pac and 185 °C for Sol-Felo) indicating the thermolability of API should not be an issue under the printing conditions used in this study.

As seen in the PXRD data (Fig. 2**a and 2b),** distinct diffraction peaks matching the peaks in the diffraction partners of the crystalline drug, but with much lower intensity can be observed in both Eud-Pac and Sol-Felo formulations after granulation indicating the presence of a low quantity of crystalline drug. Following printing, these peaks disappeared in the spectra of both formulations suggesting a transition to an amorphous solid dispersion during printing for both formulations.

ATR-FTIR data is shown in Fig. 2**c and 2d**. The Eud-Pac physical mixture showed low intensity of the peaks associated with paracetamol, most likely due to the heterogeneous sampling of the powder mixtures and the low drug loading (9.1%). ATR-FTIR granule spectra were collected on the cross-section of the granule samples, based on the findings of a previous study which found the bulk spectra to be more

representative of the granule as a whole due to non-uniform drug distributions associated with the granule drying process and the small penetration depth of the FTIR technique (1 μm) (McDonagh et al., 2022). Although the granule spectra are still dominated by the polymer carrier Eudragit E, a few small peaks associated with amorphous paracetamol are visible, including the peaks at 798 and 1508 cm^{-1}. The spectra of the Eud-Pac prints are very similar to the ones of the granules indicating amorphous paracetamol. The FTIR spectra of the Sol-Felo physical mix and granulation showed a sharp NH stretching peak at 3367 cm^{-1} indicative of crystalline felodipine polymorphic form I (Srčič et al., 1992). This peak transforms into a broad peak with low intensity in the spectra of the APF printed samples, characteristic of the amorphous form of felodipine.

Thermal transitions for the raw materials were measured using DSC shown in Fig. 2**e and 2f**. The melting peak of crystalline drug occurred at 170 °C for paracetamol and 146 °C for felodipine. Glass transition temperatures (T_g) of 56.6 °C and 70.2 °C were identified for Eudragit E PO and Soluplus, respectively, agreeing with reported literature data (Parikh et al., 2014; Alshahrani et al., 2015). The enthalpy value of the crystalline drug melting reduced significantly in the DSC result of the granules in comparison to the physical mixes for both formulations. This indicates a certain proportion of the paracetamol dissolved during the granulation process and remained amorphous after drying. This was further confirmed by the shifts of the T_g values of the granulated Eud-Pac and Sol-Felo to 41.6 °C and 53.9 °C, respectively. This reduction is most likely due to the plasticisation effects of dissolved drug on the polymers. No crystalline drug melting was detected in either of the APF printed tablet which is in agreement with the PXRD and ATR-FTIR data suggesting both printed formulations being amorphous solid dispersions.

3.2. Key quality attributes of APF printed tablets

Both granule formulations were found to be suitable for APF 3D printing directly using the processing parameters described in the method section without the need for additives, such as plasticisers. Printed tablets showed good adhesion between layers and were easily removed from the build plate with no material lose. The tablets exhibited hard plastic-like properties, were easy to handle and non-friable (the hardness of the tablets exceeded the tensile strength limit of the tablet hardness machine). This is well in-line with the literature reports on the high tensile strength values (typically greater than 10 MPa) of thermally printed tablets, such as FDM printed tablets (Wong and Hernandez, 2012), whereas the tensile strength of pressed tablets via tabletting are in the range of 1.5–2.5 MPa (Podczeck, 2012). The printability of these materials using APF is significant because like many other pharmaceutical materials Eudragit E and Soluplus lack the mechanical properties (flexibility and strength) and melt viscosities required for most thermal printing processes without using large quantities of plasticisers (McDonagh et al., 2022). Pharmaceutical material printability is one of the main hurdles limiting 3DP applications currently, therefore more versatile printing technologies such as APF,

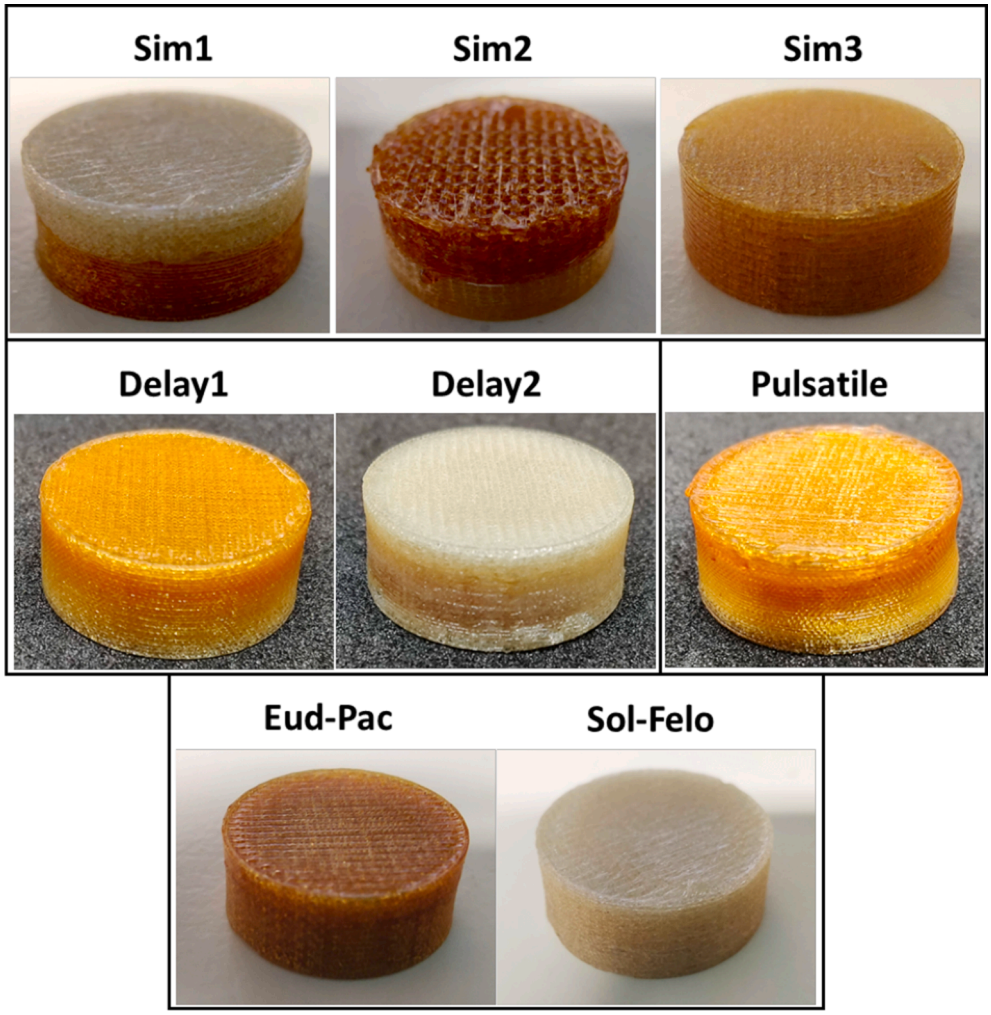

Fig. 3. Visual appearances of APF printed tablets.

which use gradual heating and extrusion under very high pressures can greatly expand the material library from which researchers can use to design novel formulations for future applications.

The visual appearances of APF printed dual-drug tablets with six different designs and two control tablets are shown in Fig. 3. Shape fidelity and weight measurements were taken for each of the tablet designs to understand the printing accuracy in term of target dimensions and shape and weight uniformity (shown in Fig. 4). Deviations from target diameter (15 mm) were minimal for all designs with all printed samples within 2% of the target diameter. Target height (6 mm) deviations were similarly low, within 3% for most designs, peaking at 5.8% for one of the Sim2 design.

Shape (diameter and height) uniformity was highly consistent (measured by the degree of variation) for all designs. Tablet mass varied dependant on design. The Sim2 design was partially porous due to the Eud-Pac half of the tablet being printed at 50% infill density resulting in it having the lowest average mass at 732 mg amongst all designs. Whilst other designs all had the same theoretical volume of deposited material, there were still variations in overall tablet mass due to the difference in density between Eud-Pac (0.85 kg/m^3) and Sol-Felo (1.10 kg/m^3) parts. For the APF printed tablet designs, all individual tablets were within 93–107% of the average mass.

3.3. Drug content

Drug content assays of printed material were measured at 100.2% ± 3.3 and 98.7% ± 1.4 of the theoretical drug load (9.1% w/w) for the Eud-Pac and Sol-Felo formulation respectively indicating no significant thermal degradation or change to API loading following granulation and printing. Both APF printed tablets showed good content uniformities, with 95.9–105.1% and 98.4–101.0% for the Eud-Pac and Sol-Felo tablets, respectively (based on data from six replicates). We recognise that the sampling of the tablets here reported does not comply to current pharmacopeia regulations of sampling twenty tablets (European Pharmacopeia 10.0., 2010), which are predicated on large scale production of tablets. 3D printing is proposed as a route to personalised medicine that will produce small batches of tailored dosage forms and will probably require new accreditation methods.

4. In vitro drug release studies of dual-drug APF printed tablets

4.1. Simultaneous release

The simultaneous release dual-drug designs all have both materials, Eud-Pac and Sol-Felo, exposed to the dissolution media during the dissolution resulting in simultaneous release of both API. Release data is shown below in Fig. 5. By first analysing the release profiles of the control tablets we can see that both formulations exhibit a pH dependant release with Eud-Pac releasing faster in the gastric phase (pH 1.2 HCl) and Sol-Felo releasing faster in the intestinal phase (pH 6.8 PBS). Eudragit E is well reported to release much faster at gastric pH (<5) due to the hydration of its dimethylamino groups, which are fully protonated at this condition (Moustafine et al., 2006; Leopold and Eikeler, 1998).

For the Sim1 tablet design drug release of both API closely matched

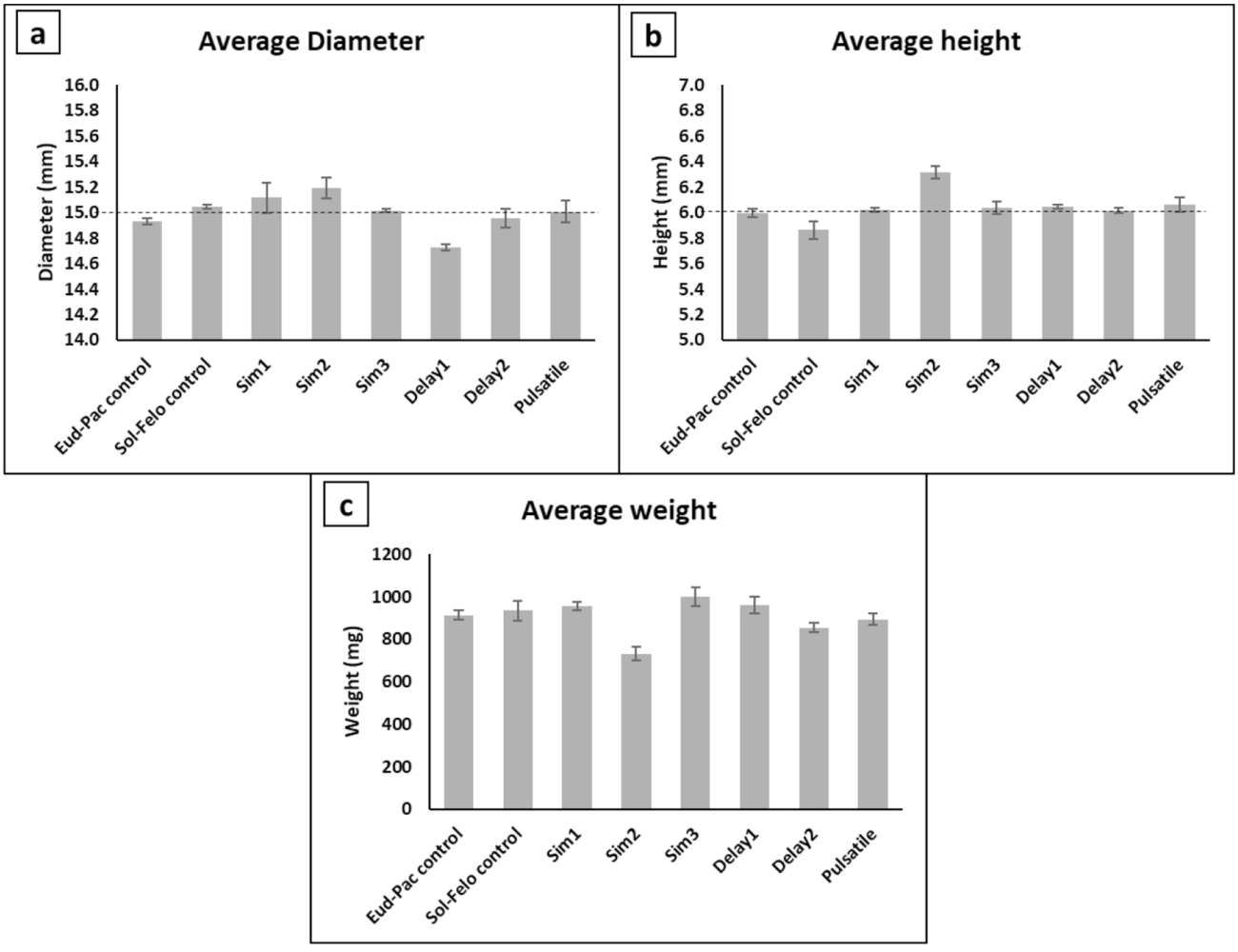

Fig. 4. Outer dimension and weight uniformiaty of the APF printed tablets. Dashed lines represent target dimensions (15 mm Diameter, 6 mm height).

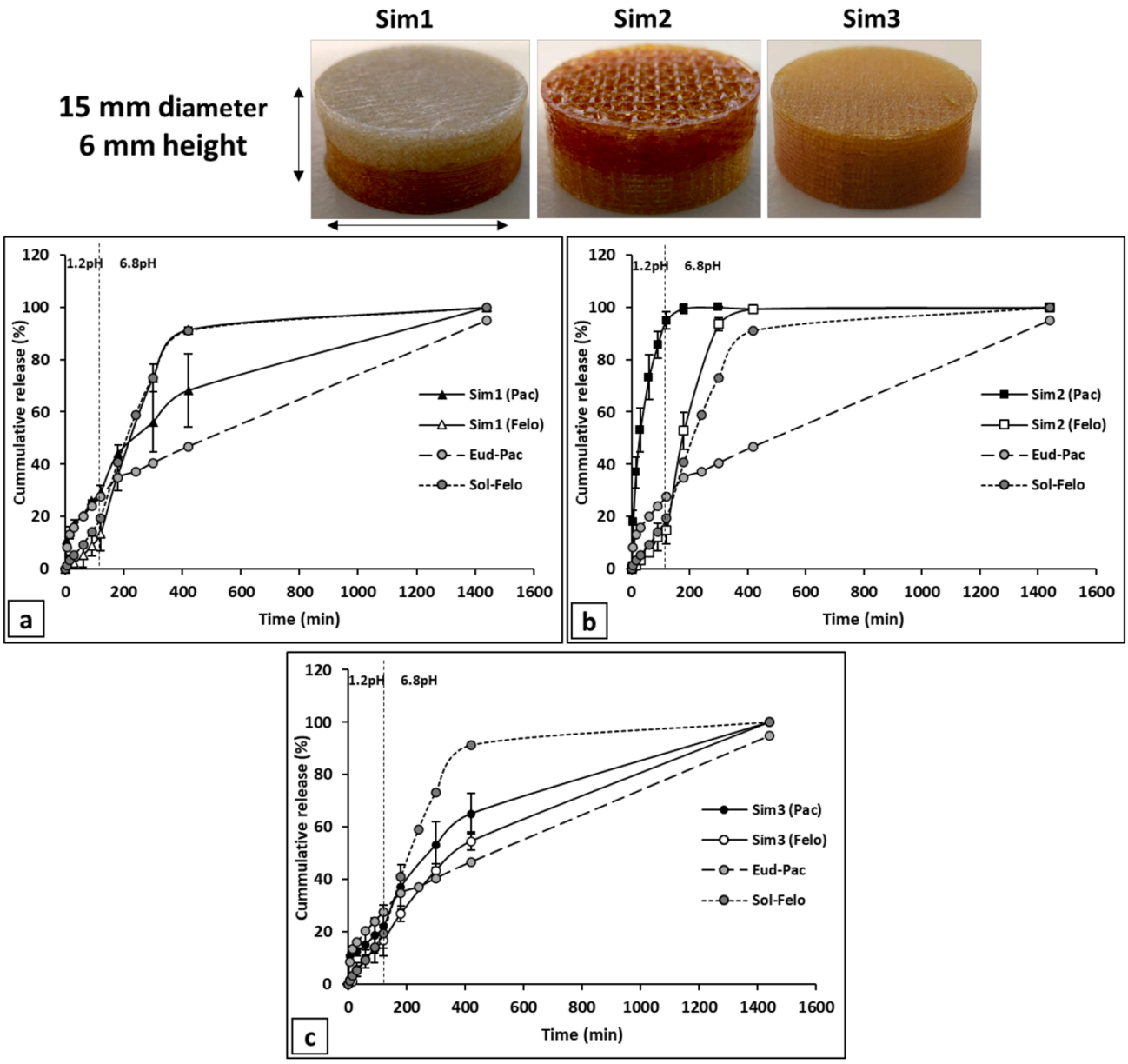

Fig. 5. In vitro drug release from simultaneous release dual-drug APF printed tablets. Cumulative paracetamol and felodipine release profiles are plotted for all designs, (a) Sim1, (b) Sim2, (c) Sim3. (The standard deviations of Eud-Pac and Sol-Felo data points are all less than 4 and 8%, respectively. They are not shown in the Figure in order to reduce the overlap with the data points of dual drug tablets).

that of the control tablets for the first 120 min at gastric pH (Fig. 5**a**). Following the dissolution media change to intestinal conditions felodipine release continued to match the control release profile whilst paracetamol release was elevated. The increased release rate after approximately 120 min compared to the control is likely attributed to the increased surface area of Eud-Pac available for dissolution at these later time points due to the more rapid erosion of the Sol-Felo tablet half. A further contributing factor may be due to the swelling properties of Soluplus which could potentially hydrate the connecting Eud-Pac half interface enabling paracetamol diffusion through the thin hydrated layer of Soluplus present towards the end of the dissolution process. Complete release of both API was achieved after 22 h.

In the Sim2 design the Sol-Felo tablet half is identical to that in Sim1 but the Eud-Pac tablet half was printed at 50% infill density. As seen with single composition tablets, the reduction in infill density was found to significantly increase the paracetamol release rate due to the increased exposed surface area of the porous structure, reaching 100% paracetamol release after approximately 2 h (Fig. 5**b**). The felodipine release profile from the non-porous half of Sim2 was initially identical to that of Sim1 and the Soluplus control but started to diverge after approximately 180 min coinciding with the complete release and erosion of the Eudragit tablet half. Once the Eud-Pac half was eroded the Sol-Felo half had another face in contact with the dissolution media increasing the exposed surface area of the tablet and thus resulting in the slightly increased release rate observed. To our knowledge this is the first-time infill density has been used in a dual-drug or polypill structure to modify release profiles.

Lastly the Sim3 drug release shown in Fig. 5**c** shows the release profiles generated when the printed material is alternated every layer (0.2 mm). Drug release from this novel design is significantly slowed compared to the Sim1 and Sim2 designs, only reaching 100% after the full 22 h. Goyanes et al printed a multilayer design with thicker 1 mm PVA layers with alternating API (Goyanes et al., 2015). They also found no significant difference in the release profiles of the two API but as a

control tablet was not included in the study it is unclear if this is a result of the multilayer design or due to using two water soluble API with the same carrier polymer. By contrast in this study, we see that Eud-Pac and Sol-Felo gave a very different pH dependent release when used as single formulations, so the sustained release profiles seen in Sim3 can be purely attributed to the pill design. The drug release profiles appear to roughly approximate the average release rates seen between the two API in the control tablets and are similar for both paracetamol and felodipine. We suspect that due to the very high aspect ratio of each layer (radius/height) the polymer layer erosion from the top and bottom tablet face is the rate limiting step causing the drug release to be mediated by the slower dissolving polymer. As such, layers of Soluplus in 1.2pH and Eudragit E in 6.8pH effectively holds up the polymer dissolution and drug release from the medial layers causing the release rate for each API to be slowed and dominated by the slower dissolving polymer. This finding indicates that such a tablet design could be useful for generating more sustained release profiles from typically fast releasing formulations and very soluble API beyond what is achievable when printing at 100% infill-density.

4.2. Delayed release

The release profiles of the Core/Shell delayed release tablet designs are shown below in Fig. 6. A few studies have explored the use of core/shell structures using different geometries and wall thicknesses/coatings as a means to control the lag time of API release and for more effective

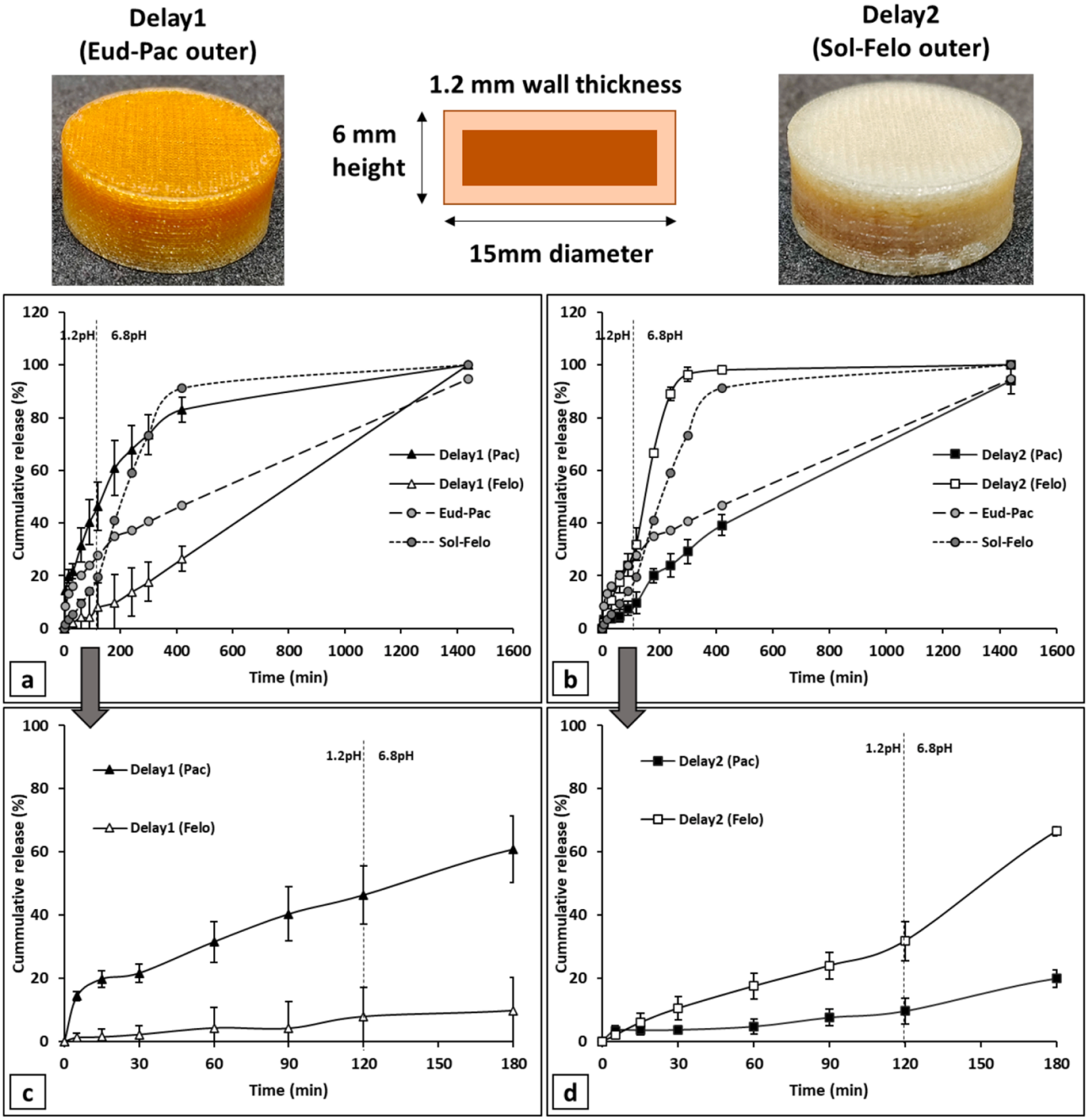

Fig. 6. In vitro drug release from delay release dual-drug APF printed tablets. Cumulative paracetamol and felodipine release are plotted for all designs, (a) Delay1, (b) Delay2, (c) the first 180 min of drug release from Delay 1, and (d) the first 180 min of drug release from Delay 2. (The standard deviations of Eud-Pac and Sol-Felo data points are all less than 4 and 8%, respectively. They are not shown in the Figure in order to reduce the overlap with the data points of dual drug tablets).

disease treatments such as hypertension (Goyanes et al., 2015; Zheng et al., 2021; Li et al., 2022). We explored the effectiveness of this design when using erodible and swellable materials. As expected, drug release was significantly slowed from the core material for both Delay1 (Eud-Pac outer material in Fig. 6**a**) and Delay2 (Sol-Felo outer material in Fig. 6**b**) tablet designs compared to the control tablets indicating the effectiveness of a solid outer shell material in delaying drug release. However, a small amount of drug release was detected at the initial time points from the core material in the Delay2 design suggesting there is some potential for the API to diffuse through the Soluplus polymer shell matrix which was 1.2 mm thick at t = 0. This could be due to the dissolution properties of Soluplus which unlike Eudragit E was observed to absorb dissolution media and swell. Eudragit E appeared to act as a better barrier layer than Soluplus with < 5% cumulative release from felodipine core in the Delay2 design at 90 min.

In both designs, drug release from the core API was significantly reduced for the initial time points compared to the control tablets due to the physical barrier provided by the outer shell. When analysing the difference between designs there is some indication that Eudragit acts as a better barrier layer (Delay1 tablet) than Soluplus (Delay2 tablet). Whilst core API release remained under 5% for the first 90 min in Delay1, for Delay2 9.3% average cumulative paracetamol release was detected indicating that a small quantity of paracetamol was able to diffuse through the 1.2 mm thick Soluplus shell. This is in spite of Eudragit E being the more soluble polymer at pH 1.2 dissolution conditions and the Delay2 shell showing minimal visible erosion at this time point. We expect this to relate to the swelling properties of Soluplus which may result in an easier network for the API to diffuse through. No distinct step change in release rate was observed, which might have been expected if the erosion of the shell material was uniform resulting in the sudden exposure of the core material. This result demonstrates that under the dynamic dissolution conditions tablet erosion is not uniform in all directions resulting in the gradual exposure of the core material and subsequently a non-defined uptick in core API release rate. When considering the release of the API in the shell material we observe elevated release rates compared to the control due to the increased surface area to volume ratio.

These results demonstrate that a simple core/shell dual-drug tablet design using erodible materials is effective for delaying and sustaining the release of the core API, but further consideration of polymer choice and shell thickness is required to create more definitive delayed release with controllable lag time.

4.3. Pulsatile release

The drug release data for the pulsatile tablet design is shown below in Fig. 7. The pulsatile tablet consisted of five layers of material in a nested design alternating between Eud-Pac and Sol-Felo with a layer thickness of 0.6 mm. Release experiments from three different pulsatile tablets have been individually plotted to clarify any possible step changes in drug release. Additionally, three horizontal dashed lines have been added to Fig. 7 at 53%, 65%, and 85% cumulative release which correspond to the theoretical amount of API in each layer of the tablet. Thus, these dashed lines indicate where the layer changes during dissolution and thus release rate step changes might be expected to occur given that the drug release is an erosion mediated process.

Between 0 and 120 min we can clearly see the initial paracetamol release from the outer Eud-Pac layer whilst almost no felodipine release was detected. This indicates the outer Eud-Pac layer was successful in delaying the release from the inner layers. This first Eud-Pac layer represents 53% of the theoretical total paracetamol content of the tablet. When 53% of cumulative paracetamol release was reached which

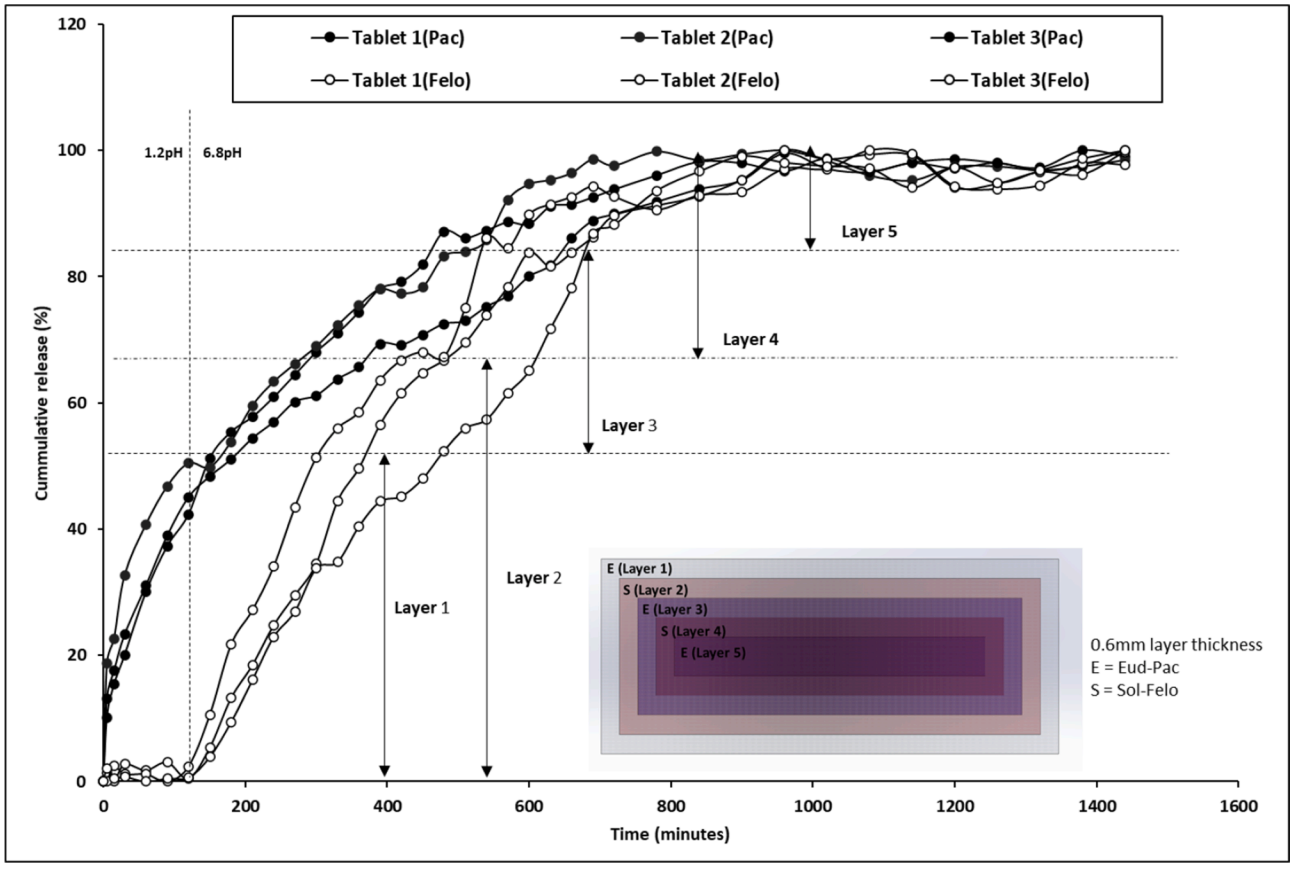

Fig. 7. In vitro drug release from three pulsatile release dual-drug APF printed tablets (named as Tablet 1, Tablet 2, Tablet 2). All tablets were with a 0.6 mm layer thickness and the layers in the insert are labelled as Layer 1–6. In the inserted tablet illustration, E stands for Eud-Pac and S stands for Sol-Felo.

occurred at approximately 120 min felodipine release began to be measured which would indicate the complete erosion and dissolution of the first layer. Following the first layer erosion the step changes in drug release due to layer erosion became significantly less defined. There are minor indications of a release rate step change at 120 min and 420 min for paracetamol and felodipine respectively, but the layer transitions are barely visible after this. After the release of the first layer at 120 min both API were seen to release simultaneously with no obvious release plateau for the more inner layers. Similar to the findings from the delayed release tablets we attribute this to the non-uniform erosion of the tablet under dynamic dissolution conditions which becomes more evident the further into the dissolution. This highlights the challenge with generating specific release profiles for multi active tablets using erodible materials. One potential solution explored in other studies is to include a barrier material between layers which would act as the rate limiting step (Khaled et al., 2015).

5. Conclusion

APF printed dual-drug tablets were successfully fabricated showing good print quality and reliability in terms of weight and content uniformity demonstrating the versatility of the APF printing process for processing non-FDM printable formulations. By precisely controlling the deposition of the Eud-Pac and Sol-Felo formulations within the tablets, simultaneous and delayed drug release profiles of both drugs in APF printed tablets were successfully generated. However, pulsatile release was not achieved due to the non-uniform erosion of the tablet under dynamic dissolution conditions. This highlights the challenge of generating intricate release profiles, especially when using an erodible system.

Key design principles of achieving independently controlled drug release from multi-drug loaded tablets can be summarised from this study. Infill density of layers loaded with different drugs, such as the Sim2 design, can be effectively used in a dual-drug tablet to independently control the drug release rate of each API. Alternating thin layer design, such as Sim3, can effectively prolong the release of the soluble drug (Pac) to match the release rate of poorly soluble drug (in this case being Felo). This alternate layer design demonstrates a simple way to reduce release rates using a software-based approach with no changes needed to feedstock or hardware. Core/shell dual-drug designs were effective in delaying the release of the core API. However, some early detection of core API in the Delay2 design highlights the importance of considering shell material and thickness. In summary, these results give further insight into the types of dual-drug tablet designs which can be used to create complex multi-API release profiles for more effective personalised medication. A wider variety of polymers should be further tested to confirm whether the design principles can be generalised to polymers with similar physicochemical properties.

CRediT authorship contribution statement

Thomas McDonagh: Methodology, Validation, Formal analysis, Investigation, Conceptualization, Data curation, Project administration, Visualization, Writing – original draft, Writing – review & editing. **Peter Belton:** Methodology, Validation, Formal analysis, Supervision, Investigation, Writing – review & editing. **Sheng Qi:** Conceptualization, Methodology, Formal analysis, Investigation, Resources, Data curation, Visualization, Supervision, Project administration, Funding acquisition, Writing – review & editing.

Declaration of Competing Interest

The authors declare that they have no known competing financial interests or personal relationships that could have appeared to influence the work reported in this paper.

Data availability

Data will be made available on request.

Acknowledgement

We would like to thank the Enabling Innovation: Research to Application (EIRA), a Research England Connecting Capability Fund (CCF) project for providing the funding for the study. Additional thanks to Arburg for their Freeformer training and material qualification insight as well as PCE Automation for their technical support.

References:

Alayoubi, A., Zidan, A., Asfari, S., Ashraf, M., Sau, L., Kopcha, M., 2022. Mechanistic understanding of the performance of personalized 3D-printed cardiovascular polypills: A case study of patient-centered therapy. Int. J. Pharm. 617, 121599.

S.M. Alshahrani, J.-B. Lu W Fau - Park, J.T. Park Jb Fau - Morott, B.B. Morott Jt Fau - Alsulays, S. Alsulays Bb Fau - Majumdar, N. Majumdar S Fau - Langley, K. Langley N Fau - Kolter, A. Kolter K Fau - Gryczke, M.A. Gryczke A Fau - Repka, M.A. Repka, Stability-enhanced hot-melt extruded amorphous solid dispersions via combinations of Soluplus® and HPMCAS-HF. AAPS PharmSciTech. 2015 Aug;16(4):824-34. doi: 10.1208/s12249-014-0269-6. Epub 2015 Jan 8.

Bangalore, S., Shahane, A., Parkar, S., Messerli, F.H., 2007. Compliance and fixed-dose combination therapy. Curr. Hypertens. Rep. 9, 184–189.

Boniatti, J.; Januskaite, P.; Fonseca, L.B.d.; Viçosa, A.L.; Amendoeira, F.C.; Tuleu, C.; Basit, A.W.; Goyanes, A.; Ré, M.-I. Direct Powder Extrusion 3D Printing of Praziquantel to Overcome Neglected Disease Formulation Challenges in Paediatric Populations. Pharmaceutics 2021, 13, 1114. https://doi.org/10.3390/pharmaceutics13081114.

Chew, S.A., Arriaga, M.A., Hinojosa, V.A., 2016. Effects of surface area to volume ratio of PLGA scaffolds with different architectures on scaffold degradation characteristics and drug release kinetics. J. Biomed. Mater. Res. A 104 (5), 1202–1211.

Cui, M., Pan, H., Fang, D., Sun, H., Qiao, S., Pan, W., 2021. Exploration and evaluation of dynamic dose-control platform for pediatric medicine based on Drop-on-Powder 3D printing technology. Int. J. Pharm. 596, 120201.

Dumpa, N.R., Sarabu, S., Bandari, S., Zhang, F., Repka, M.A., 2018. Chronotherapeutic drug delivery of Ketoprofen and Ibuprofen for improved treatment of early morning stiffness in arthritis using hot-melt extrusion Technology. AAPS Pharm. Sci. Tech. 19 (6), 2700–2709.

Gao, J., Chen, C., Chen, J.-X., Wen, L.-M., Yang, G.-L., Duan, F.-P., Huang, Z.-Y., Li, D.-F., Yu, D.-R., Yang, H.-J., 2014. Synergism and rules of the new combination drug Yiqijiedu formulae (YQJD) on ischemic stroke based on amino acids (AAs) metabolism. Sci. Rep. 4, 1–11.

Goh, W.J., Tan, S.X., Pastorin, G., Ho, P.C.L., Hu, J., Lim, S.H., 2021. 3D printing of four-in-one oral polypill with multiple release profiles for personalized delivery of caffeine and vitamin B analogues. Int. J. Pharm. 598, 120360.

Goyanes, A., Wang, J., Buanz, A., Martínez-Pacheco, R., Telford, R., Gaisford, S., Basit, A. W., 2015. 3D Printing of Medicines: Engineering Novel Oral Devices with Unique Design and Drug Release Characteristics. Mol. Pharm. 12, 4077–4084.

Goyanes, A., Allahham, N., Trenfield, S.J., Stoyanov, E., Gaisford, S., Basit, A.W., 2019. Direct powder extrusion 3D printing: Fabrication of drug products using a novel single-step process. Int. J. Pharm. 567, 118471 https://doi.org/10.1016/j.ijpharm.2019.118471.

Heer, D., Aggarwal, G., Kumar, S.L.H., 2013. Recent trends of fast dissolving drug delivery system–an overview of formulation technology. Pharmacophore 4, 1–9.

Herrada-Manchón, H., Rodríguez-González, D., Alejandro Fernández, M., Suñé-Pou, M., Pérez-Lozano, P., García-Montoya, E., Aguilar, E., 2020. 3D printed gummies: Personalized drug dosage in a safe and appealing way. Int. J. Pharm. 587, 119687.

Khaled, S.A., Burley, J.C., Alexander, M.R., Yang, J., Roberts, C.J., 2015. 3D printing of five-in-one dose combination polypill with defined immediate and sustained release profiles. J. Control. Release 217, 308–314.

Khaled, S.A., Burley, J.C., Alexander, M.R., Yang, J., Roberts, C.J., 2015. 3D printing of tablets containing multiple drugs with defined release profiles. Int. J. Pharm. 494, 643–650.

Korte, C., Quodbach, J., 2018. 3D-printed network structures as controlled-release drug delivery systems: dose adjustment, API release analysis and prediction. AAPS PharmSciTech 19, 3333–3342.

Leopold, C.S., Eikeler, D., 1998. Eudragit E as coating material for the pH-controlled drug release in the topical treatment of inflammatory bowel disease (IBD). J. Drug Target 6 (2), 85–94.

R. Li, Y. Pan, D. Chen, X. Xu, G. Yan, T. Fan, Design, Preparation and In Vitro Evaluation of Core–Shell Fused Deposition Modelling 3D-Printed Verapamil Hydrochloride Pulsatile Tablets, in: Pharmaceutics, 2022.

Mandal, A.S., Biswas, N., Karim, K.M., Guha, A., Chatterjee, S., Behera, M., Kuotsu, K., 2010. Drug delivery system based on chronobiology—A review. J. Control. Release 147, 314–325.

Martinez, P.R., Goyanes, A., Basit, A.W., Gaisford, S., 2018. Influence of geometry on the drug release profiles of stereolithographic (SLA) 3D-printed tablets. AAPS PharmSciTech 19, 3355–3361.

McDonagh, T., Belton, P., Qi, S., 2022. Direct granule feeding of thermal droplet deposition 3D printing of porous pharmaceutical solid dosage forms free of plasticisers. Pharm. Res. 1–12.
McDonagh, T., Belton, P., Qi, S., 2022. An investigation into the effects of geometric scaling and pore structure on drug dose and release of 3D printed solid dosage forms. Eur. J. Pharm. Biopharm.
Moustafine, R.I., Zaharov, I.M., Kemenova, V.A., 2006. Physicochemical characterization and drug release properties of Eudragit® E PO/Eudragit® L 100–55 interpolyelectrolyte complexes. Eur. J. Pharm. Biopharm. 63, 26–36.
Parikh, T., Gupta, S.S., Meena, A., Serajuddin, A., 2014. Investigation of thermal and viscoelastic properties of polymers relevant to hot melt extrusion - III: Polymethacrylates and polymethacrylic acid based polymers. Journal of Excipients and Food Chemicals 5, 56–64.
Pasina, L., Brucato, A.L., Falcone, C., Cucchi, E., Bresciani, A., Sottocorno, M., Taddei, G. C., Casati, M., Franchi, C., Djade, C.D., Nobili, A., 2014. Medication Non-Adherence Among Elderly Patients Newly Discharged and Receiving Polypharmacy. Drugs Aging 31, 283–289.
Podczeck, F., 2012. Methods for the practical determination of the mechanical strength of tablets—From empiricism to science. Int. J. Pharm. 436, 214–232.
Power of one, 2019. what is holding polypills back? Pharm. J. 303.
Robles-Martinez, P., Xu, X., Trenfield, S.J., Awad, A., Goyanes, A., Telford, R., Basit, A. W., Gaisford, S., 2019. 3D Printing of a Multi-Layered Polypill Containing Six Drugs Using a Novel Stereolithographic Method. Pharmaceutics 11.
M.C.S. Rodrigues, C.d. Oliveira, Drug-drug interactions and adverse drug reactions in polypharmacy among older adults: an integrative review, Revista latino-americana de enfermagem, 24 (2016).
Roshandel, G., Khoshnia, M., Poustchi, H., Hemming, K., Kamangar, F., Gharavi, A., Ostovaneh, M.R., Nateghi, A., Majed, M., Navabakhsh, B., Merat, S., Pourshams, A., Nalini, M., Malekzadeh, F., Sadeghi, M., Mohammadifard, N., Sarrafzadegan, N., Naemi-Tabiei, M., Fazel, A., Brennan, P., Etemadi, A., Boffetta, P., Thomas, N., Marshall, T., Cheng, K.K., Malekzadeh, R., 2019. Effectiveness of polypill for primary and secondary prevention of cardiovascular diseases (PolyIran): a pragmatic, cluster-randomised trial. Lancet 394, 672–683.
Sánchez-Guirales, S.A., Jurado, N., Kara, A., Lalatsa, A., Serrano, D.R., 2021 Sep 29. Understanding Direct Powder Extrusion for Fabrication of 3D Printed Personalised Medicines: A Case Study for Nifedipine Minitablets. Pharmaceutics. 13 (10), 1583. https://doi.org/10.3390/pharmaceutics13101583. PMID: 34683875; PMCID: PMC8537449.
Saydam, M., Takka, S., 2020. Improving the dissolution of a water-insoluble orphan drug through a fused deposition modelling 3-Dimensional printing technology approach. Eur. J. Pharm. Sci. 152, 105426.
Srčič, S., Kerč, J., Urleb, U., Zupančič, I., Lahajnar, G., Kofler, B., Šmid-Korbar, J., 1992. Investigation of felodipine polymorphism and its glassy state. Int. J. Pharm. 87, 1–10.
T.I.P. Study, Effects of a polypill (Polycap) on risk factors in middle-aged individuals without cardiovascular disease (TIPS): a phase II, double-blind, randomised trial, The Lancet, 373 (2009) 1341-1351.
Triastek, 2015. URL https://www.triastek.com. (accessed 12.11.22).
Uniformity of content of single-dose preparations, in, European Pharmacopeia 10.0, 2010.
Vaz, V.M., Kumar, L., 2021. 3D Printing as a Promising Tool in Personalized Medicine. AAPS PharmSciTech 22, 49.
Von Zeppelin, D., Manka, M., 2017. ARBURG plastic freeforming. Engineering of Biomaterials 20.
Wiley, B., Fuster, V., 2014. The concept of the polypill in the prevention of cardiovascular disease. Ann. Glob. Health 80, 24–34.
Wong, K.V., Hernandez, A., 2012. A review of additive manufacturing. International Scholarly Research Notices 2012.
Yang, Y., Wang, H., Xu, X., Yang, G., 2021. Strategies and mechanisms to improve the printability of pharmaceutical polymers Eudragit® EPO and Soluplus®. Int. J. Pharm. 599, 120410.
Zhang, J., Feng, X., Patil, H., Tiwari, R.V., Repka, M.A., 2017. Coupling 3D printing with hot-melt extrusion to produce controlled-release tablets. Int. J. Pharm. 519, 186–197.
Zhang, B., Gleadall, A., Belton, P., McDonagh, T., Bibb, R., Qi, S., 2021. New insights into the effects of porosity, pore length, pore shape and pore alignment on drug release from extrusionbased additive manufactured pharmaceuticals. Addit. Manuf. 46, 102196.
Zhang, B., Nasereddin, J., McDonagh, T., von Zeppelin, D., Gleadall, A., Alqahtani, F., Bibb, R., Belton, P., Qi, S., 2021. Effects of porosity on drug release kinetics of swellable and erodible porous pharmaceutical solid dosage forms fabricated by hot melt droplet deposition 3D printing. Int. J. Pharm. 604, 120626.
Zhang, B., Teoh, X.Y., Yan, J., Gleadall, A., Belton, P., Bibb, R., Qi, S., 2022. Development of combi-pills using the coupling of semi-solid syringe extrusion 3D printing with fused deposition modelling. Int. J. Pharm. 625, 122140.
Zhang, J., Yang, W., Vo, A.Q., Feng, X., Ye, X., Kim, D.W., Repka, M.A., 2017. Hydroxypropyl methylcellulose-based controlled release dosage by melt extrusion and 3D printing: Structure and drug release correlation. Carbohydr. Polym. 177, 49–57.
Zheng, Y., Deng, F., Wang, B., Wu, Y., Luo, Q., Zuo, X., Liu, X., Cao, L., Li, M., Lu, H., Cheng, S., Li, X., 2021. Melt extrusion deposition (MED™) 3D printing technology – A paradigm shift in design and development of modified release drug products. Int. J. Pharm. 602, 120639.